Microbuckling instability in elastomeric cellular solids

Rosakis, P., Ruina, A., and Lakes, R. S.,
"Microbuckling instability in elastomeric cellular solids",
J. Materials Science, 28, 4667-4672 (1993).

R. Lakes[§], P. Rosakis[*] and A. Ruina[*]

[§]Department of Engineering Physics
Engineering Mechanics Program; Biomedical Engineering Department
Materials Science Program and Rheology Research Center
University of Wisconsin-Madison
1500 Engineering Drive, Madison, WI 53706-1687
USA

[*] Department of Theoretical and Applied Mechanics
Cornell University
Ithaca, NY 14853
USA

Abstract

Compressive properties of elastic cellular solids are studied via experiments upon foam and upon single cell models. Open cell foam exhibits a monotonic stress-strain relation with a plateau region; deformation is localized in transverse bands. Single cell models exhibit a force-deformation relation which is not monotonic. In view of recent concepts of the continuum theory of elasticity, the banding instability of the foam in compression is considered to be a consequence of the non-monotonic relation between force and deformation of the single cell.

1. Introduction

Cellular solids are currently used in many structural applications. It is therefore of interest to understand as fully as possible the physical mechanisms for deformation and damage formation. With sufficient understanding we consider it to be possible to develop new cellular solids with superior resistance to damage.

Elastomeric foams are known to exhibit several regions of behavior in simple uniaxial compression: (i) approximately linear behavior for strains less than about 0.05, (ii) a plateau region in which strain increases at constant or nearly constant stress, and (iii) a densification region of the stress strain curve in which its slope increases markedly with strain. This behavior is roughly explained as follows. Linear elasticity arises from bending of the cell ribs, plateau arises from their elastic buckling, and densification arises from contact between ribs [1]. Simple analytical models based on elastic buckling of the ribs have been used in an effort to predict the behavior of foams. They indicate a value of strain at which the transition between linear elasticity and plateau regions occurs to be about 0.05, which corresponds closely with experiment [1].

Ductile foams such as those made of metals also exhibit regions of linear elasticity, plateau, and densification. In ductile foams, the plateau region is associated with plastic buckling of cell ribs rather than elastic buckling. Moreover, in elastomeric foams rib buckling is fully reversible (though accompanied by hysteresis) while in ductile foams, rib buckling is associated with permanent microdamage.

The purpose of this paper is to advance the understanding of compressive collapse in cellular solids with the aid of the theory of stability of elastic continua. Since elastomeric foams are more representative of elastic continua than are ductile foams, we consider here rib microbuckling of elastomeric foams and its relation to elastic stability of the foam as a whole. Ductile foams, which are more important in applications requiring the support of relatively large stress are not considered here.

2. Materials and methods

Scott Industrial Foam, which is a reticulated, open cell polyurethane foam, was examined experimentally to determine mechanical properties. The pore size was 1.3 mm (20 pores per inch). Macroscopic models of individual cells were also prepared from rods of polyurethane rubber, 6.1 mm in diameter. Open cell models in the shape of a tetrakaidecahedron (with ribs 25 mm long) and a regular octahedron (with ribs 50 mm long) were made. The tetrakaidecahedron has six faces in the shape of squares and eight faces in the shape of regular hexagons (Fig. 1); it is considered representative of typical cells in foams.

Mechanical testing was conducted using a servohydraulic testing machine (Instron, Canton, MA, model 1321) at room temperature (71°F, 55% relative humidity). The specimens were mounted between rigid platens and held by friction in compression tests. Some tests of compression and tension were done with the specimen cemented to the platens with cyanoacrylate adhesive. Several trials were also conducted in which compression specimens were lubricated with silicone spray lubricant. Long blocks of foam in compression tests were restrained laterally on one or two surfaces to prevent macroscopic buckling. Some torsion tests upon square cross section bars were done as well, however the interpretation of such tests is less simple than for compression as a result of the inhomogeneous strain field in torsion of a bar. The foam was examined visually and under low power magnification during deformation. The tetrakaidecahedron model was loaded in compression upon a pair of square faces and a pair of hexagonal faces in separate tests. The octahedron model was loaded upon a pair of triangular faces and a pair of vertices in separate tests. Tests of successive loading and unloading were performed at constant platen displacement rates in displacement control (triangular waveforms at 0.033 to 0.0033 cycle/sec) corresponding to periods from 30 to 300 seconds. Strains presented in the graphs were calculated from the platen displacement signal.

3. Experimental results

Uniaxial compression of blocks of Scott Industrial Foam of different size and shape resulted in the stress strain curves shown in Fig. 2. Observe that the curves are monotonic. The results for a large block longer than its width agree with those of Choi and Lakes [2]. Further experiments upon compression specimens which were lubricated or cemented to the platens disclosed similar behavior. The overall shape of the curves was insensitive to changes in strain rate. A small block, also longer than its width behaved similarly to the large one, as shown in Fig. 2.

Bands of localized deformation were observed visually, and they were transverse to the direction of compression. The bands contained cells which were highly compressed to the point of contact between adjacent ribs. The bands were of low contrast. The bands began to form when the gage length of the specimen reached a strain of about 0.1, and were very evident at a strain of 0.2. Further compression within the plateau region of strain resulted in an increase in the number of bands, until they occupied most of the specimen, at which point macroscopic densification occurred. The band thickness depended on the cell size; the bands were several cells thick in foam of cell size 0.4 mm and in foam of cell size 1.2 mm. We remark that banding localization is known to occur in the tensile loading of polymers and metals beyond the yield point, and in plastic deformation of ductile honeycombs [3]. In the case of the present polymer foam, the banding localization was completely reversible, i.e. the bands disappeared upon the removal of load.

The foams exhibited considerable hysteresis, both in loading from zero into the densification region and in loading over a restricted range of deformation. In the latter case, a measure Δ of hysteresis loss was defined as the ratio of the hysteresis loop width in load to the total excursion in load. In linear viscoelasticity the hysteresis loop is elliptical and the above ratio is $\sin \delta$ in which δ is the loss angle δ. For strain excursions of 0.09 peak to peak, $\Delta = 0.11$ for excursions about zero; $\Delta = 0.24$ in the plateau region ($\varepsilon = 0.2$ to 0.43), and $\Delta = 0.19$ in the densification region ($\varepsilon = 0.73$).

Compressive behavior of a stubby block, shorter in the load direction than its width, differed from the above in that there was essentially no plateau region, as shown in Fig. 2. The behavior of thin layer of foam, about two cells thick, cemented to rigid platens was similar to that of the stubby block.

The compressive behavior of the tetrakaidecahedron cell model was *not* monotonic, as shown in Fig. 3, in contrast to the behavior of the foam as a whole. The load-deformation curve displayed *negative slope* over a range of strain; outside this range the slope was positive. The curve had this shape regardless whether the compression load was applied to the square faces or the hexagonal faces. An octahedron cell model also exhibited a non-monotonic load-deformation curve of similar shape to the above. The tetrakaidecahedron single cell model behaved similarly to the foam in that the region of approximately linear behavior was of similar extent, densification began to occur at about the same strain, and rib alignment in tension caused a similar nonlinearity. The principal difference is the presence or failure of monotonicity in the 'plateau' region. During compression, the tetrakaidecahedron cell model first bulged outward in the transverse directions, then assumed a biconcave shape, then ribs came in contact resulting in a rapid increase in stress.

Torsion tests upon a square cross section foam specimen disclosed load deformation curves with slopes which varied smoothly by a small amount. There were no abrupt changes in slope nor were there plateau regions. Torsion of a specimen under precompression of 24% or tension of 37% axial strain had no dramatic effect on the shape of the load deformation curve. No localization in the form of bands were observed in any torsion test.

As for foam materials with negative Poisson's ratios [4, 5.], prior study disclosed the absence of a plateau region in the stress strain curves. In the present study compressed specimens of negative Poisson's ratio material were examined for a banding instability, however none was found.

4. Considerations of stability in elastic continua

The experimental observation of band formation in the compression of foams is considered to be a manifestation of elastic instability. To aid in the interpretation of the results, we present salient aspects of the theory of stability in elastic continua.

4.1. Linear elasticity

There are several ranges of elastic constants which are associated with stability on various levels. We consider first the case of linear isotropic elasticity. The strain energy is positive definite if and only if the shear modulus G and Poisson's ratio ν satisfy

$$G>0 \text{ and } -1<\nu<0.5 \qquad (1)$$

or equivalently, $G>0$ and $3\lambda+2G>0$ in which λ and G are the Lamé constants.

Materials which obey these relations give rise to unique solutions of boundary value problems in which either surface traction or surface displacements are specified. Moreover, such materials are stable to small macroscopic perturbations.

Displacement type boundary value problems have unique solutions if [6]

$$G>0 \text{ and } -\infty<\nu<0.5 \text{ and } 1<\nu<\infty \qquad (2)$$

This range is considerably less restrictive than Eq. 1. Moreover, other ranges for uniqueness can be obtained for specific boundary shapes.

The conditions for strong ellipticity are [7]

$$G>0 \text{ and } \lambda+2G>0, \qquad (3)$$

equivalent to Eq. 2 above; see also Eq. 4.

If strong ellipticity is violated, the material may exhibit an instability associated with the formation of bands of inhomogeneous deformation [7]. The physical significance of the $\lambda+2G>0$ condition of strong ellipticity is that the stiffness is positive for axial compression or extension under lateral constraint (uniaxial *strain*) , as is the speed of longitudinal waves. Eq. 3 is equivalent to [8]

$$G>0, \frac{E(1-\nu)}{(1+\nu)(1-2\nu)} = 2G\frac{(1-\nu)}{(1-2\nu)} > 0 \qquad (4)$$

in which E is Young's modulus, or

$$G>0 \text{ and } \nu<0.5 \text{ or } \nu>1 \qquad (5)$$

Since $E=2G(1+\nu)$, the range of E for strong ellipticity is $-\infty < E < \infty$. As for the bulk modulus,

$$B = \frac{2G(1+\nu)}{3(1-2\nu)} \qquad (6)$$

or equivalently $B = \lambda + 2G/3$, so that for strong ellipticity $-4G/3 < B < \infty$. However as implied by Eq. 1, E, G, and B must be positive for positive definiteness of the strain energy and for the material to be *globally* stable under small deformation.

In summary, we observe that conditions for global stability of an elastic solid and local stability (with respect to the formation of bands) are not identical.

4.2. Nonlinear elasticity

In a one-dimensional nonlinearly elastic bar the condition for strong ellipticity is that

$$\frac{d^2W}{d\lambda^2} > 0, \qquad (7)$$

in which the material in question has a strain energy density $W(\lambda)$ where λ is the stretch ratio (equal to $1 + \varepsilon$) with ε the engineering strain. Inequality (7) is equivalent to $d\sigma/d\lambda > 0$ with σ as the Piola (engineering) stress. That is, the stress strain curve is monotonically increasing in uniaxial strain.

Failure of ellipticity may occur in the form of a change of sign in the slope of the stress strain curve; the slope may become negative over an interval of strain. This was predicted [9] to result in localized deformation in the form of bands of material under high strain. Another prediction of the theory is that while the local (microscopic) stress-strain curve has regions of negative slope, the macroscopic load-elongation response observed will always have a nonnegative slope.

In three dimensions, the strain energy density $W(\lambda_1,\lambda_2,\lambda_3)$ depends nonlinearly on the three principal stretch ratios λ_1, λ_2, λ_3. Necessary and sufficient conditions of strong ellipticity (hence stability with respect to localized-strain band formation) are rather complicated [10]; see also [7] for a two-dimensional analysis). For the special case of uniaxial stress, along the λ_1 direction, the lateral stretches are equal: $\lambda_2(\lambda_1) = \lambda_3(\lambda_1)$. The three-dimensional conditions for strong ellipticity reduce to

$$\frac{\lambda_1\sigma_1}{(\lambda_1^2 - \lambda_2^2)} > 0 \qquad (8)$$

$$\frac{\partial^2 W}{\partial \lambda_1^2} > 0, \frac{\partial^2 W}{\partial \lambda_2^2} > 0, \frac{\partial^2 W}{\partial \lambda_3^2} > 0 \qquad (9)$$

$$\frac{\lambda_1\sigma_1}{(\lambda_1^2 - \lambda_2^2)} + \left(\frac{\partial^2 W}{\partial \lambda_1^2}\frac{\partial^2 W}{\partial \lambda_2^2}\right)^{1/2} > \left|\frac{\partial^2 W}{\partial \lambda_1 \partial \lambda_2} + \frac{\lambda_2\sigma_1}{(\lambda_1^2 - \lambda_2^2)}\right| \qquad (10)$$

in which $\sigma_1 = \partial W/\partial\lambda_1$ is the stress in the axial direction. We remark that Eq's 9 are analogous to Eq. 7 in one dimension.

5. Analysis of experiment

The bands which develop in compressed foam are indicative of failure of ellipticity of the material viewed as a continuum. The non-monotonic compressive load deformation behavior of single cell models is regarded as a causal mechanism for the macroscopic behavior of the foam in the plateau region and for the banding instability.

5.1. Detailed analysis for one dimension

To understand the formation of bands, consider a one-dimensional nonlinear elastic bar with strain energy density $W(\lambda)$ in which λ is the stretch ratio $\lambda = 1 + \varepsilon$ with ε the engineering strain. The stress in the bar is $\sigma = dW(\lambda)/d\lambda$. Suppose that on the continuum level, the stress-strain curve (equivalent to a stress-stretch curve following a shift on the abscissa) is as shown in Fig. 4. This behavior is qualitatively similar to the pressure-volume relation considered responsible for the liquid-vapor phase transition. The plateau region in the foam stress-strain curve is analogous to isothermal expansion at constant pressure of a liquid-vapor mixture.

Equilibrium requires σ = constant along the bar. It can be shown [9] that values of the stretch in an interval $\lambda_M < \lambda < \lambda_m$ where $d^2W/d\lambda^2 < 0$ are unstable, hence are physically unobservable. For values of applied stress in the range $\sigma_M < \sigma < \sigma_m$ (between the local minimum and maximum of the stress-stretch curve in Fig. 4), there are two possible values λ of corresponding to the same σ, excluding the unstable middle region; these may be called λ_+ and λ_-. For values of stress outside that interval there is a unique stretch corresponding to a uniform strain solution. In the theory of nonlinear elasticity one can model phase changes by allowing strain discontinuities while maintaining continuous displacements [9, 11, 7, 12]. In the present setting it is possible to have a discontinuity in strain. The regions of different strain (or stretch) correspond to the *bands* of localized compression observed in the experiments. The stretch is discontinuous along the bar, alternating between the values λ_+ and λ_-. The average stretch λ_{avg} must obey the relation $\lambda_- < \lambda_{avg} < \lambda_+$ so there is a constraint on the amount of material in each kind of region.

We now consider the shape of the *macroscopic* response curve. Under the above assumptions the macroscopic response (in which stress vs average stretch is observed) is not unique but can take the form of any curve within CBDE in Fig. 4 [12]. This non-uniqueness may be removed by making additional assumptions. For example, if one assumes that the bar undergoes deformations such that its total potential energy is minimized [9, 11] while satisfying the boundary conditions, the macroscopic response exhibits a flat *plateau* region, line q-q in Fig. 4, at the 'Maxwell stress' [9]. This stress is determined by requiring the areas between the macroscopic and microscopic response to be equal. This response is reversible and there is no hysteresis. The macroscopic response coincides with the microscopic stress-stretch curve over the monotonically increasing portions FEq and qBA in Fig. 4. In the context of the cellular solids examined here, the theory predicts that a non-monotonic microscopic response (or single cell response since we do not have a continuum) gives rise to a monotonically nondecreasing macroscopic response with a *plateau*.

A nonzero slope in the plateau region (such as is observed experimentally) is predicted theoretically under the assumption of inhomogeneity in the bar [11]. The microscopic response shown in Fig. 4 differs in its details from point to point in the bar but the curve always has the same shape. In the foams this inhomogeneity is associated with small density variations throughout the foam, and variations in the buckling loads of cells depending on their geometry and orientation.

The hysteresis observed in the experiments may be explained in part by assuming an energy cost associated with movement of the edges of bands [12]. Physically, we consider that a portion of this energy dissipation arises from the friction between cell ribs during collapse of the cells. Such analysis does not account for the hysteresis which is observed in regions other than the plateau region. A more complete analysis would incorporate the viscoelasticity of the foam material.

The width of the bands was observed to depend on the cell size. However, the classical theory of elasticity has no characteristic length scale and so cannot account for such effects. Length scales can be incorporated via Cosserat elasticity or via theories which incorporate strain gradients [13, 14, 15].

It is noteworthy that this analysis predicts a macroscopic response to be caused by a markedly different microscopic response (in a continuum sense). The latter corresponds to the experimentally observed behavior of a physical single foam cell model.

5.2 Analysis for three dimensions

The experiments were done upon three-dimensional specimens. Analysis of the three dimensional situation is therefore called for. In the uniaxial stress compression test of an isotropic material with a positive Poisson's ratio we have $\lambda_2 = \lambda_3 > \lambda_1$ and the applied compressive stress $\sigma_1 < 0$ so that Eq. 10 is always true. Since the lateral surfaces in this experiment were free, $\sigma_2 = \partial W(\lambda_1,\lambda_2(\lambda_1),\lambda_3(\lambda_1))/\partial\lambda_2 = 0$, and similarly for σ_3. Differentiating with respect to λ_1,

$$\partial^2 W/\partial\lambda_1\partial\lambda_2 = - [\partial^2 W/\partial\lambda_2{}^2 + \partial^2 W/\partial\lambda_2\partial\lambda_3][\partial\lambda_2/\partial\lambda_1] \qquad (11)$$

We also have $\sigma_1 = \partial W(\lambda_1,\lambda_2(\lambda_1),\lambda_3(\lambda_1))/\partial\lambda_1$. Differentiating with respect to λ_1,

$\partial\sigma_2(\lambda_1)/\partial\lambda_1 = \partial^2W/\partial\lambda_1^2 - 2[\partial^2W/\partial\lambda_2^2 + \partial^2W/\partial\lambda_2\partial\lambda_3][\partial\lambda_2/\partial\lambda_1]^2$ (12)

We used the experimental results of Choi and Lakes [2] for Poisson's ratio vs strain to generate a plot of $\lambda_2(\lambda_1)$vs λ_1. The curve attained a relative maximum at $\lambda_1 \approx 0.85$, at which $\lambda_2 \approx 1.03$ and $\partial\lambda_2/\partial\lambda_1 = 0$. At this point in $(\lambda_1,\lambda_2,\lambda_3)$ space, assuming $\partial^2W/\partial\lambda_2^2 > 0$ (otherwise Eq. 9 fails), Eq. 11 gives $\partial^2W/\partial\lambda_1\partial\lambda_2 = 0$ and $d\sigma_1(\lambda_1)/d\lambda_1 > 0$. Then Eq. 10 reduces to

$$\frac{\sigma_1}{(\lambda_1 - \lambda_2)} + [\frac{d\sigma_1}{d\lambda_1}\frac{\partial^2W}{\partial\lambda_2^2}] > 0 \qquad (13)$$

The first term is negative. A perfectly flat plateau corresponds to $d\sigma_1/d\lambda_1 = 0$ and therefore to failure of ellipticity. Ellipticity may also fail in the presence of a sufficiently small but positive slope in the plateau region, depending on the value of $\partial^2W/\partial\lambda_2^2$ in contrast to the conclusions from the one-dimensional analysis, however we do not have an experimental value of this derivative.

5.3 Discussion

Open cell foam exhibits a monotonic stress-strain relation with a plateau region; deformation is localized in transverse bands. Single cell models exhibit a force-deformation relation which is not monotonic. The difference between the single cell response and the 'continuum' response of foam is understood in terms of stability analysis of the foam considered as an elastic continuum. Related analysis of localization of strain in porous media has been conducted [16]. The present study, however, presents a non-monotonic force-deformation relation for the single cell as an experimentally evaluated causal mechanism for the overall foam behavior.

6. Conclusions

1 Open cell foam exhibits a monotonic stress strain relation with a plateau region; deformation is localized in transverse bands of material under higher compressive strain.

2 Single cell models exhibit a force-deformation relation which is not monotonic in compression.

3 The behavior of the single cell models is viewed as the cause of the banding localization and the plateau effect.

Acknowledgment

Partial support by the NASA/ Boeing ATCAS program under contract #NAS1-18889, and by a University Faculty Scholar Award from the University of Iowa to R. Lakes is gratefully acknowledged. This research was conducted while R. Lakes was at the Department of Theoretical and Applied Mechanics at Cornell University. P. Rosakis wishes to acknowledge the support of the National Science Foundation through Grant # MSS-9009730.

References

1. Gibson, L.J. and Ashby, M.F. *Cellular solids*, (Pergamon, 1988).
2. Choi, J. B. and Lakes, R. S., "Nonlinear properties of polymer cellular materials with a negative Poisson's ratio", J. Materials Science, 27, 4678-4684 (1992).
3. Stronge, W.J. and Shim, V.P.W. "Microdynamics of crushing in cellular solids", J. Engineering Materials Technology 110, 185-190, 1988.
4. Lakes, R.S. "Foam structures with a negative Poisson's ratio", Science, 235. 1038-1040 1987
5. Friis, E.A., Lakes, R.S., and Park, J.B., "Negative Poisson's ratio polymeric and metallic materials", Journal of Materials Science, 23, 4406-4414, 1988.
6. Bramble, J.H. and Payne, L.E., "On the uniqueness problem in the second boundary value problem in elasticity", Proc. fourth National Congress of Applied Mechanics, 469-473, 1963.
7. Knowles, J. K. and Sternberg, E. "On the failure of ellipticity and the emergence of discontinuous gradients in plane finite elastostatics", J. Elasticity 8, 329-379, 1978.

8. Timoshenko S. P. and Goodier, J. N., *Theory of elasticity*, McGraw-Hill, 3rd edition, (1970).
9. Ericksen, J. L., "Equilibrium of bars", J. Elasticity, 5, 191-201, 1975.
10. Simpson, H. C. and Spector, S. J., "On copositive matrices and strong ellipticity for isotropic elastic materials", Arch. Rational Mech. Analy. 84, 55-68, 1983.
11. James, R. D., "Co-existent phases in one-dimensional static theory of elastic bars", Arch. Rational Mech. Analy. 72, 100-140, 1979.
12. Abeyaratne, R. and Knowles, J. K., "On the dissipative response due to discontinuous strains in bars of unstable elastic material", Int. J. Solids, Structures, 24, 1021-1044, 1988.
13. Gurtin, M. E., "The gradient theory of phase transitions on a finite interval", in Phase transformations and material instabilities in solids, ed. M. E. Gurtin, Academic, NY, 1984.
14. Lakes, R. S., "Experimental methods for conventional and negative Poisson's ratio cellular solids as Cosserat solids", ASME J. Engineering Materials and Tech. 113, 1313, 1990.
15. Mühlhaus, H. B. and Aifantis, E. C., "A variational principle for gradient plasticity", Int. J. Solids, Structures, in press.
16. Abeyaratne, R. and Triantafyllidis, N. "An investigation of localization in a porous elastic material using homogenization theory", J. Applied Mechanics, 51, 481-486, 1984.

Figures

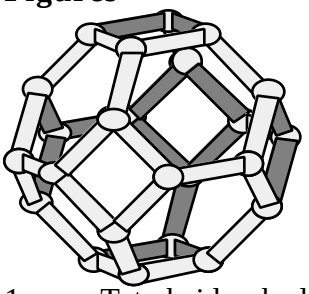

1 Tetrakaidecahedron cell model. Actual model made from rubber rods.

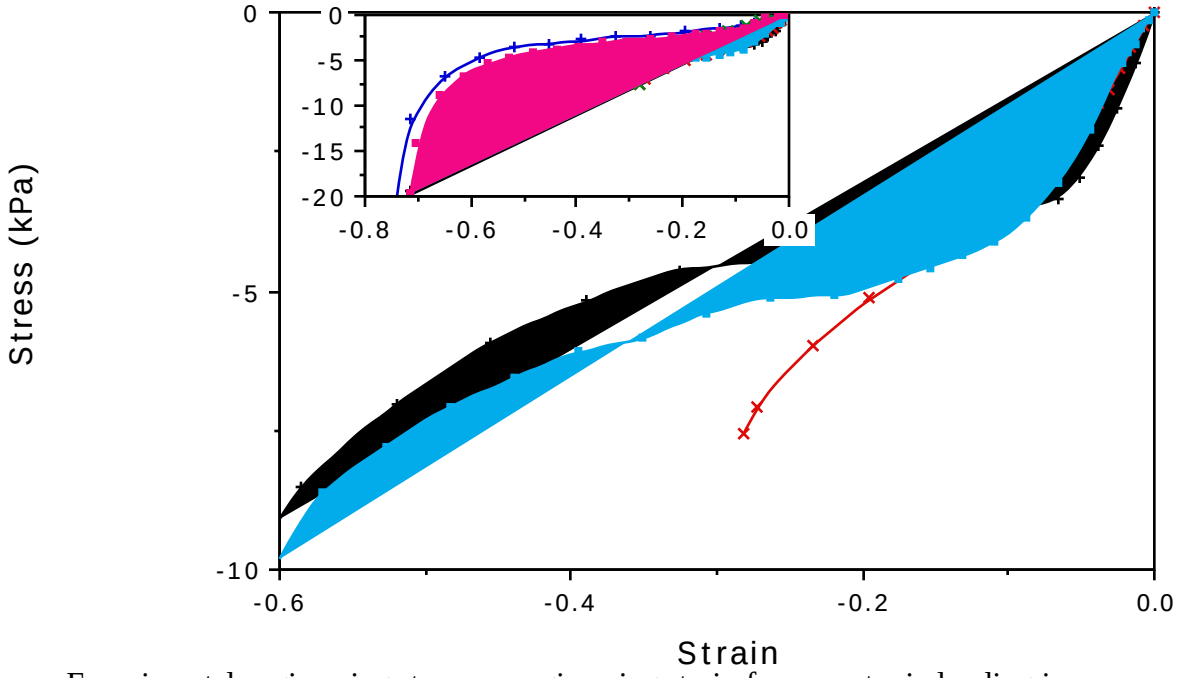

2 Experimental engineering stress vs engineering strain for monotonic loading in compression for Scott Industrial Foam, 20 pore/inch.
sq Block 52 mm by 53 mm by 121 mm long
\+ Block 15 mm by 15 mm by 19 mm long
x Stubby Block 52 mm by 53 mm by 19 mm long
Inset: Stress-strain curves shown on a wider strain scale and including hysteresis during loading and unloading; same symbols as large graph.

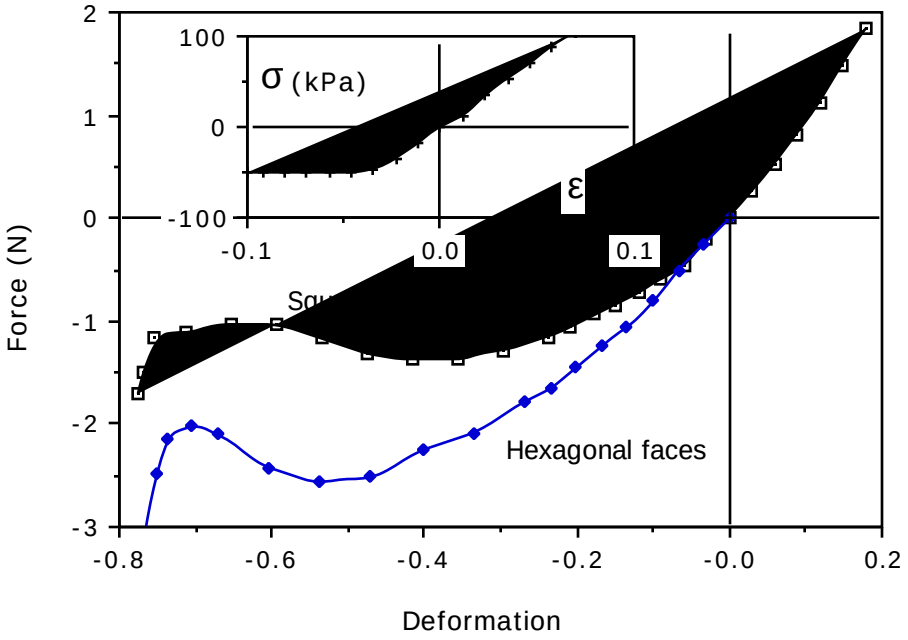

3 Experimental axial force vs deformation (calculated as change in cell width divided by original cell width) for tetrakaidecahedral cell model with ribs 25 mm long and 6 mm in diameter.

Inset: engineering stress vs strain (ΔL/L) for a single rib. Plateau in compression corresponds to buckling and postbuckling.

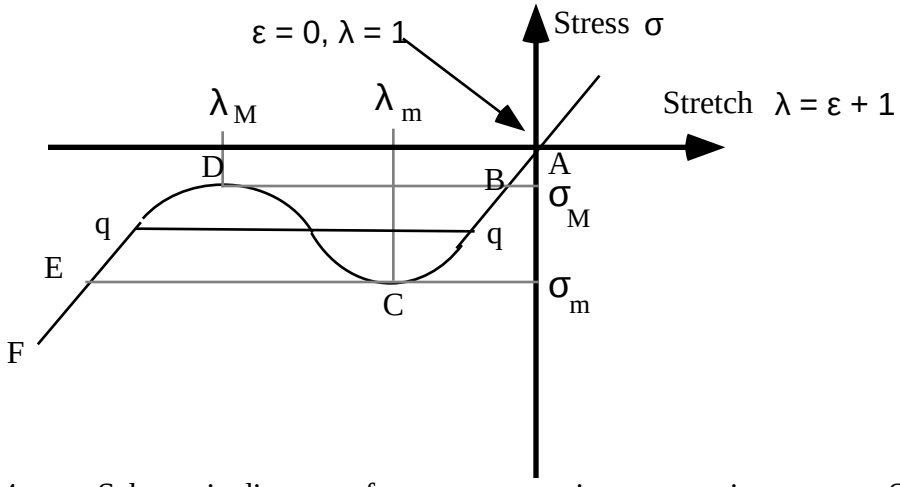

4 Schematic diagram of a non-monotonic stress strain response. Symbols are as used in text.